Eur. Phys. J. C (2024) 84:802
https://doi.org/10.1140/epjc/s10052-024-13162-1

THE EUROPEAN PHYSICAL JOURNAL C

Regular Article - Theoretical Physics

Comprehensive study of bouncing cosmological models in $f(Q,T)$ theory

M. Zeeshan Gul[a], **M. Sharif**[b], **Shamraiza Shabbir**[c]

Department of Mathematics and Statistics, The University of Lahore, 1-KM Defence Road, Lahore 54000, Pakistan

Received: 24 May 2024 / Accepted: 22 July 2024

Abstract The main objective of this article is to investigate the viability of bouncing cosmological scenarios using different forms of scale factors with perfect matter configuration in the framework of extended symmetric teleparallel theory. This modified proposal is defined by the function $f(Q,T)$, where Q characterizes non-metricity and T denotes the trace of energy-momentum tensor. We investigate the modified field equations of this theory using different parametric values of the Hubble parameter and non-metricity to derive viable solutions. These solutions are relevant in various cosmological bounce models such as symmetric-bounce, super-bounce, oscillatory-bounce, matter-bounce and exponential-bounce models. Furthermore, we examine the behavior of energy density and pressure to analyze the characteristics of dark energy. A comprehensive analysis is also conducted to explore the behavior of the equation of state parameter and deceleration parameter to examine the evolutionary eras of the cosmos. Our findings show that the $f(Q,T)$ gravity describes the cosmic expansion in the vicinity of the bouncing point during the early and late times of cosmic evolution.

1 Introduction

Einstein's general theory of relativity (EGTR) revolutionized our understanding of gravity and spacetime, which plays a crucial role in modern physics. It has been studied extensively through observations and experiments on the basis of complex shapes and measurements in space known as Riemannian geometry. Weyl [1] provided a comprehensive description of gravitational fields and matter using a more general framework than Riemann's space with the aim to unify electromagnetic and gravitational forces. The Levi-Civita connection plays a vital role in the Riemann space by comparing vector's length [2,3]. However, Weyl proposed an alternative connection that does not consider the magnitude of vectors during parallel transport. To address this limitation, he introduced a second connection referred to as the length connection which focuses on adjusting or measuring the conformal factor without considering the movement of vector's direction. Beyond Riemannian geometry, non-Riemannian geometries provide more comprehensive representations of spacetime curvature incorporating torsion (turning or rotation) and non-metricity (variation from metric compatibility). Weyl's theory considers non-metricity through covariance derivative of the metric tensor that is not equal to zero [4]. Various extended theories of gravity in different context has been discussed in [5–14].

The non-metricity offers a different cosmological model in the absence of dark energy (DE). The incorporation of non-metricity into gravitational theory is driven by a range of mathematical and physical factors. One compelling reason arises from the geometric explanation of the non-metricity associated with the metric tensor. The concept of non-metricity involves the alteration in the length of a vector as it undergoes during parallel transport which offers the important insights into the geometric characteristics of spacetime. There is a growing interest among researchers in investigating the geometry which involves the non-metricity, particularly the $f(Q,T)$ theory for multiple reasons including its theoretical consequences, alignment with observational data and its importance in cosmic scenarios [15]. This theory presents a new geometric understanding of spacetime by introducing the non-metricity as a fundamental quantity. This extended theory incorporates the trace of energy-momentum tensor (EMT) in the functional action of symmetric teleparallel theory and effectively accounts the cosmic accelerated expansion. Researchers are increasingly interested in explor-

[a] e-mail: mzeeshangul.math@gmail.com
[b] e-mail: msharif.math@pu.edu.pk (corresponding author)
[c] e-mail: shamraiza.math@gmail.com

Published online: 12 August 2024

ing various aspects of this theory. Arora et al. [16] examined the characteristics of DE in this theory using different constraints on the model parameters. The same authors [17] analyzed that this theory offers a novel approach in understanding the dark sector of the cosmos. The geometry of compact stars with different considerations in $f(Q)$ and $f(Q,T)$ theory has been studied in [18–23].

Singh and Lalke [24] studied the cosmological implications using hyperbolic solutions in the context of this theory. Their key findings demonstrated that this modified theory provides a mechanism for explaining the accelerated expansion of the cosmos. Xu and his colleagues [25] examined the dynamics of the universe in the extended symmetric teleparallel theory and compared the obtained results with ΛCDM model. Gadbail and his co-authors [26] uncovered important cosmological insights in this modified framework and determined how this theory demonstrates the cosmic phenomena. Narawade et al. [27] analyzed the cosmic acceleration through various cosmographic parameters in the same theory. Bourakadi et al. [28] demonstrated that this theory yields significant consequences in the formation and evolution of black holes. Shekh [29] investigated late-time cosmic acceleration through newly developed scale factor for the FRW model in this theory. The cosmic acceleration through deceleration parameter in this context has been studied in [30]. Sharif and Ibrar [31] explored the reconstruction of a ghost dark energy model in this context.

Bouncing cosmology offers a compelling approach to addressing solutions for initial singularity issues [32–35]. This concept aims to resolve the challenges associated with the big bang singularity, which is a significant problem in cosmology. The fundamental idea behind bouncing cosmology is to propose a model where the universe does not originate from a singular point (as theorized by the big bang), but instead undergoes a contraction followed by a bounce that leads to its current expansion. This model helps to avoid theoretical complications and infinite values resulting from singularities, offering a smooth and more accurate explanation of the cosmic origin and its dynamic properties. Furthermore, cosmic bounce has been investigated in [36], which addresses several issues of the early cosmos such as flatness problem, horizon problem and initial singularity.

The investigation of bouncing cosmology in different modified theories has gained significant attention due to its fascinating characteristics. Ilyas and Rahman [37] explored the FRW model in $f(R)$ gravity that addresses the big bang singularity through bouncing cosmology. Shamir [38] examined the viable bouncing solutions in the framework of $f(G,T)$ gravity, where G is Gauss-Bonnet invariant. Stability of the closed Einstein universe and Noether symmetry approach in the modified famework has been discussed in [39–43]. Zubair et al. [44] found that the matter-bounce models exhibit stability only for linear forms of $f(R,T)$ function while the reconstructed solutions show instability for the power law model. The same authors [45] investigated bouncing cosmology in the framework of $f(\mathcal{T},T)$ gravity, ($\mathcal{T}$ represents the torsion) by examining cosmographic parameters. Ganiou et al. [46] used the reconstruction approach to analyze the specific $f(G)$ gravity models that describe the critical phases of the cosmic evolution. Singh et al. [47] explored a bouncing scenario in $f(R,T)$ gravity using parametrization of the Hubble parameter. Their results offer valuable insights into a cosmological model where the universe undergoes a bounce, highlighting a key features such as singularity avoidance, phantom divide crossing and extreme dynamics near the bouncing point. Houndjo et al. [48] discussed the bouncing cosmology in the context of $f(\mathcal{T})$ theory. Sharif et al. [49] investigated the bouncing cosmology in the framework of $f(Q)$ gravity using a reconstruction approach with perfect matter configuration.

This paper is organized as follows. Section 2 outlines the fundamental formulation of $f(Q,T)$ gravity. A detailed examination of different types of bouncing solutions are presented in Sect. 3. In order to evaluate the bouncing cosmos, we calculate the solution to gravitational field equations using a different parametrization of scale factor. Additionally, we discuss the graphical behavior of cosmic parameters including scale factor, Hubble parameter, fluids parameter and EoS parameter. In Sect. 4, we examine the behavior of the deceleration parameter and analyze the energy conditions, redshift parameter to assess the viability of a non-singular bounce. Our main findings are summarized in Sect. 5.

2 $f(Q,T)$ theory and FRW universe model

The corresponding integral action is defined as [15]

$$S=\frac{1}{2}\int f(Q,T)\sqrt{-g}d^4x+\int \mathcal{L}_m\sqrt{-g}d^4x. \tag{1}$$

The non-metricity is given by

$$Q=-g^{\gamma\beta}(L^{\alpha}_{\ \sigma\gamma}L^{\sigma}_{\ \beta\alpha}-L^{\alpha}_{\ \sigma\alpha}L^{\sigma}_{\ \gamma\beta}), \tag{2}$$

where the disformation tensor is defined as

$$L^{\varphi}_{\ \alpha\zeta}=-\frac{1}{2}g^{\varphi\delta}\big(\nabla_{\zeta}g_{\alpha\delta}+\nabla_{\alpha}g_{\delta\zeta}-\nabla_{\delta}g_{\alpha\zeta}\big). \tag{3}$$

The superpotential is expressed as

$$P^{\alpha}_{\zeta\lambda}=-\frac{1}{2}L^{\alpha}_{\zeta\lambda}+\frac{1}{4}(Q^{\alpha}-\tilde{Q}_{\alpha})g_{\zeta\lambda}-\frac{1}{4}\delta^{\alpha}_{\ (\zeta}Q_{\lambda)}. \tag{4}$$

The relation for non-metricity using superpotential is given by

$$\begin{aligned}Q&=-Q_{\alpha\zeta\lambda}P^{\alpha\zeta\lambda}\\&=-\frac{1}{4}\big[-Q^{\alpha\zeta\lambda}Q_{\alpha\zeta\lambda}+2Q^{\alpha\zeta\lambda}Q_{\lambda\alpha\zeta}-2Q^{\varphi}\tilde{Q}_{\varphi}+Q^{\varphi}Q_{\varphi}\big].\end{aligned} \tag{5}$$

The corresponding field equations are

$$T_{\alpha\beta} = -\frac{1}{2} f g_{\alpha\beta} - \frac{2}{\sqrt{-g}} \nabla^{\zeta} (f_Q \sqrt{-g} P_{\zeta\alpha\beta}) - f_Q (P_{\zeta\alpha\lambda} Q_{\beta}{}^{\zeta\lambda} - 2Q^{\zeta\lambda}{}_{\alpha} P_{\zeta\lambda\beta}) + f_T (T_{\alpha\beta} + \theta_{\alpha\beta}). \tag{6}$$

Here, f_Q and f_T represent the derivatives corresponding to non-metricity and trace of EMT, respectively.

We consider a flat FRW universe model with scale factor $a(t)$ as

$$ds^2 = dt^2 - a^2(t)(dx^2 + dy^2 + dz^2). \tag{7}$$

The isotropic matter configuration is given by

$$T_{\alpha\beta} = (\rho + p) u_\alpha u_\beta - p g_{\alpha\beta}, \tag{8}$$

where ρ, p and u_α represent the energy density, pressure and four-velocity of the fluid, respectively. Using Eqs. (6)–(8), the resulting field equations are

$$\rho = -\frac{1}{2} f - 6H^2 f_Q - f_T (\rho + p), \tag{9}$$

$$p = \frac{1}{2} f + 2 f_Q \dot{H} + 2H f_{QQ} + 6H^2 f_Q, \tag{10}$$

with

$$Q = -6H^2, \quad T = \rho - 3p. \tag{11}$$

Here, $H = \frac{\dot{a}}{a}$ is the Hubble parameter and dot demonstrates the derivative with respect to time. These field equations are in complex form due to the involvement of multivariate functions and their derivatives. To address this challenge, we consider a specific model as

$$f(Q, T) = \xi_1 Q + \xi_2 T, \tag{12}$$

to simplify the field equations and obtain explicit expressions for energy density and pressure. Here, ξ_1 and ξ_2 are non-zero arbitrary constants. Numerous studies have been conducted on this model in the literature [50]. This model considers a linear relationship between non-metricity and trace of EMT, helping us to understand the gravitational phenomena and allows for more accurate solutions. Consequently, it is regarded as a valuable theoretical framework to comprehend the fundamental principles of gravitational physics and carries importance for both theoretical analysis and practical applications. The corresponding field equations are

$$\rho = \frac{1}{6\xi_2} [4\xi_1 \xi_2 \dot{H} + 6\xi_1 H^2 - 18\xi_1 \xi_2 H^2], \tag{13}$$

$$p = \frac{1}{9\xi_2} [12\xi_1 \xi_2 (4\xi_1 \dot{H} + 6\xi_1 H^2) - 18\xi_1 \xi_2^2 H^2 + 4\xi_1 \xi_2^2 \dot{H} + 6\xi_1 \xi_2 H^2]. \tag{14}$$

In the following sections, we explore the behavior of various bouncing models, providing valuable insights into the structure of cosmic evolution.

3 Bouncing models

This section examines the viability of various bouncing models like symmetric-bounce, super-bounce, oscillatory-bounce, matter-bounce and exponential-bounce II due to their intriguing properties. This approach enables us to determine the gravitational model based on a selected cosmological framework which can be derived using different forms of scale factors and Hubble parameters [51]. To obtain a comprehensive analysis, it is crucial that the above bounce models must represent the dynamical behavior throughout various cosmic eras. This can be achieved by analyzing different ranges of the parametric values to reconstruct different cosmic epochs [52]. Different types of bouncing model are outlined below.

3.1 Evolution of symmetric-bounce model

This model was first examined by Cai et al. [53] to formulate the non-singular bounce after an ekpyrotic contraction phase. The idea of a symmetric-bounce is based on the notion that the cosmos undergoes a phase of contraction from the previous state of expansion, reaching a minimum size (bounce point) and then starts to expand again. The term symmetric in this context refers to the behavior of the cosmological dynamics during the contraction and expansion phases. This concept is significant in theoretical cosmology, bouncing universe scenario and other modified gravity theories. These models attempt to address cosmological challenges such as the nature of the big bang singularity and the origin of the cosmos [54]. We consider the extended symmetric bouncing cosmology characterized by scale factor as [55]

$$a = \mathbb{A}\, e^{\frac{\eta t^2}{t_\star^2}}, \tag{15}$$

where $t_\star$ and t are an arbitrary and cosmic time, $\mathbb{A}$ and η are positive constants. However, the cosmic time is measured in gigayears (Gyr). Understanding the evolution of the scale factor is essential to comprehend how the universe expands, contracts or undergoes a bouncing phase. The scale factor is a positive function that quantifies the change in size of the cosmos, representing its dynamics over time. The graphical behavior of scale factor is shown in the left plot of Fig. 1 which shows a positive symmetric pattern, indicating that the scale factor decreases and increases in a balanced manner on either side of the bouncing point.

Using Eq. (15), the Hubble parameter and non-metricity become

$$H = \left(\frac{2\eta t}{t_\star}^2\right), \quad Q = -\frac{24\eta^2 t^2}{t_\star^2}. \tag{16}$$

The right plot of Fig. 1 demonstrates that the Hubble parameter is zero at bouncing point ($t = 0$) as well as shows con-

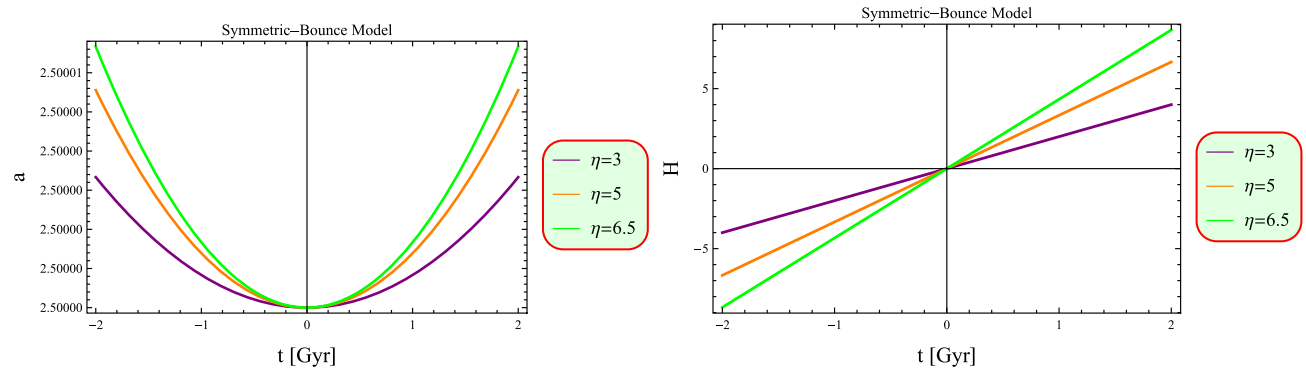

Fig. 1 Behavior of scale factor and Hubble parameter versus cosmic time

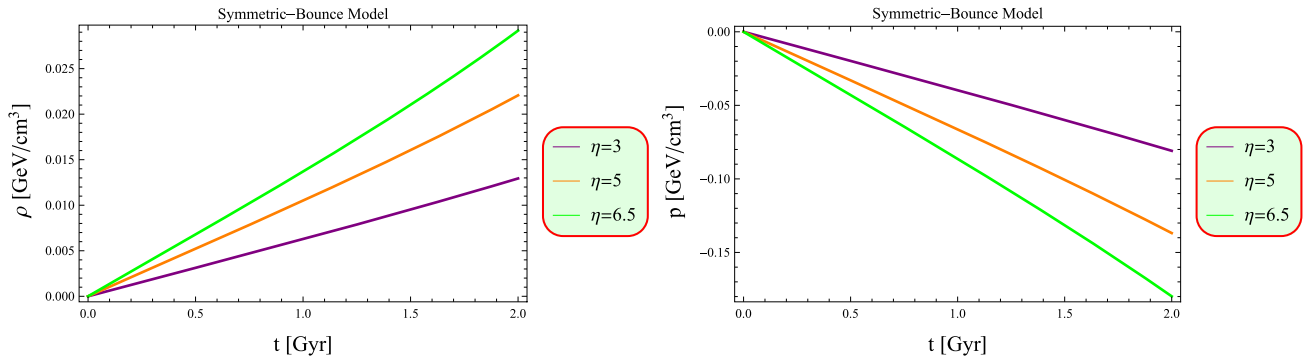

Fig. 2 Behavior of density and pressure corresponding to cosmic time

traction before the bounce ($t < 0$) and expansion after the bounce ($t > 0$). Using Eq. (16) into Eqs. (13)–(14), we obtain

$$\rho = \frac{4t\eta\xi_1\Big(-3t(2t^2+1)\eta(\xi_2-7)+t_\star\xi_2\Big)}{t_\star(2\xi_2^2-49)}, \tag{17}$$

$$p = \frac{1}{t_\star^2(2\xi_2^2-49)}\Big[4t\eta\xi_1\big(3t(2t^2+1)\eta(\xi_2+7) + t_\star(3\xi_2+14)\big)\Big]. \tag{18}$$

The units for energy density and pressure are considered as GeV/cm^3. Figure 2 shows the variation in density and pressure for symmetric-bounce model. The graphical behavior demonstrates that the energy density exhibits an positively increasing trend and pressure displays negatively downward trajectory over time. This inverse relationship between energy density and pressure is in accordance with the expected behavior predicted by the DE model.

The EoS parameter ($\omega = \frac{p}{\rho}$) can be classified based on different stages of cosmic evolution. One can obtain matter-dominated eras such as dust, radiative fluid and stiff matter for $\omega = 0,\ \frac{1}{3},\ 1$, respectively, whereas, the vacuum, phantom and quintessence phases of the cosmos are characterized by $\omega = -1,\ \omega < -1,\ -1 < \omega < -\frac{1}{3}$, respectively [56]. Using Eqs. (17) and (18), we calculate the value of the EoS parameter for symmetric-bounce model as

$$\omega = -\frac{3\eta(\xi_2+7)\big(2t^3+t\big)+(3\xi_2+14)t_\star}{3\eta(\xi_2-7)t\big(2t^2+1\big)-\xi_2 t_\star}. \tag{19}$$

Figure 3 shows that the EoS parameter becomes singular at the bounce point and undergoes rapid evolution in the vicinity of the bounce. During this period, the EoS parameter exhibits symmetry around the epoch of the bounce and transitions into the phantom region ($\omega < -1$). This behavior indicates a significant shift in the characteristics of this parameter as the system approaches and moves towards the bouncing point. In the context of cosmology, such a bounce represents a critical phase where the cosmos shows transition from a contracting state to an expanding one.

3.2 Analysis of super-bounce model

The concept of super-bounce is characterized by a power-law scale factor which was first proposed in [57]. The idea of a super-bounce suggests that the cosmos undergoes cycles of expansion and contraction, rather than a single expansion followed by infinite expansion without encountering a singularity. The general form of the scale factor is defined as

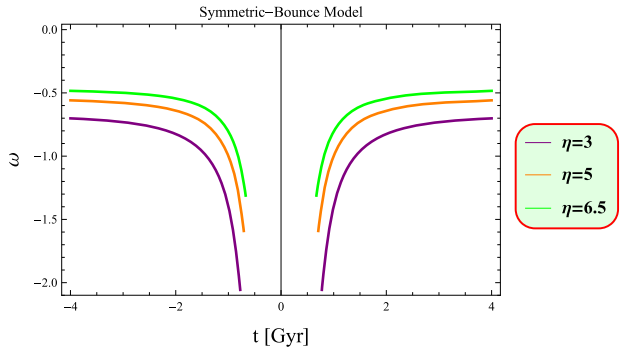

Fig. 3 Behavior of EoS parameter for different parametric values

$$a = e^{\left(\frac{t_b - t}{t_0}\right)^{\frac{2}{\mathbb{Z}^2}}}, \tag{20}$$

where $\mathbb{Z} > 3$, $t_0 > 0$ and t_b denotes the time of the bounce event. The graphical behavior of the super-bounce scale factor is shown in the left plot of Fig. 4. The graph indicates that the scale factor is positive, but does not show a symmetric pattern in this model on either side of the bouncing point. The corresponding value of the Hubble parameter and non-metricity become

$$H = -\frac{2}{\mathbb{Z}^2}\left(\frac{1}{t_b - t}\right), \quad Q = \frac{24}{\mathbb{Z}^4}\left(\frac{1}{t_b - t}\right)^2. \tag{21}$$

In the right plot of Fig. 4 demonstrates the behavior of the Hubble parameter in super-bounce with distinct characteristics before and after the bouncing point. This parameter changes its signatures during the transition phase of contraction/ expansion and becomes singular at $H = 0$. This indicates a critical phase, where the dynamics of the cosmos undergoes a significant transformation. Using Eq. (21) in Eqs. (13)–(14), we have

$$\rho = -\frac{1}{\mathbb{Z}^4(t - t_b)^2(2\xi_2^2 - 49)}\left[2\xi_1\left((\mathbb{Z}^2 + 18)\xi_2 - 126\right)\right], \tag{22}$$

$$p = -\frac{1}{\mathbb{Z}^4(t - t_b)^2(2\xi_2^2 - 49)(3\xi_2 - 14)} \times\left[36\xi_1\left(\left(\xi_2(5\xi_2 - 7) + 98\right) + 7\mathbb{Z}^2(\xi_2^2 - 28)\right)\right]. \tag{23}$$

Figure 5 depicts the graphical representation of fluid parameters for the super-bounce model, which are closely resemble those obtained in the symmetric-bounce model and are consistent with behavior of the DE model. We use Eqs. (22) and (23) to determine the EoS parameter value for super-bounce model as

$$\omega = \frac{1}{(3\xi_2 - 14)\left(\xi_2(\mathbb{Z}^2 + 18) - 126\right)}\left[18\xi_2(7 - 5\xi_2) + 98\right) + 7\mathbb{Z}^2(\xi_2^2 - 28)\Big]. \tag{24}$$

Figure 6 shows that the behavior of EoS parameter is identical as obtain in symmetric-bounce model. This means that the physical conditions governing the cosmic behavior is stable and does not reach infinite values at any point during the bounce which ensures a smooth transition through this critical phase.

3.3 Evolution of oscillatory-bounce model

The concept of an oscillatory-bounce is significant in the field of cosmology and scenarios involving the expansion and contraction of the cosmos. In this bouncing scenario, the cosmos undergoes a periodic cycles of expansion and contraction. Each cycle initiates with a big bang followed by a phase of expansion and concludes with a big crunch, where the cosmos contracts back to a dense state before beginning with another big bang. This cyclic pattern implies a repetitive sequence of cosmic events alternating between expansion and contraction over successive cycles [58]. The corresponding expression for the scale factor is expressed as

$$a = \mathbb{A}\sin^2\left(\frac{\mathbb{B}t}{t_\star}\right), \tag{25}$$

where $\mathbb{A}$ and $\mathbb{B}$ are non-negative constants. In the left side of Fig. 7 shows the graphical behavior of scale factor

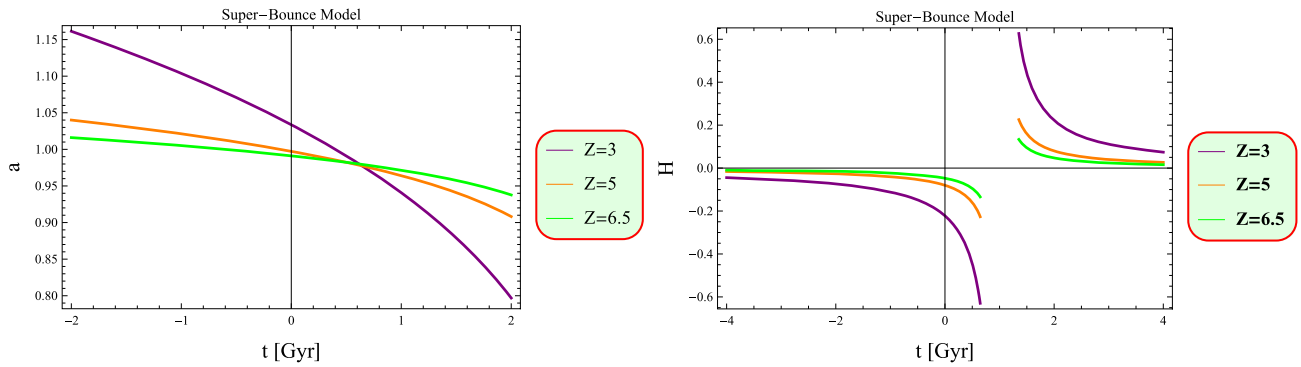

Fig. 4 Behavior of scale factor and Hubble parameter versus cosmic time

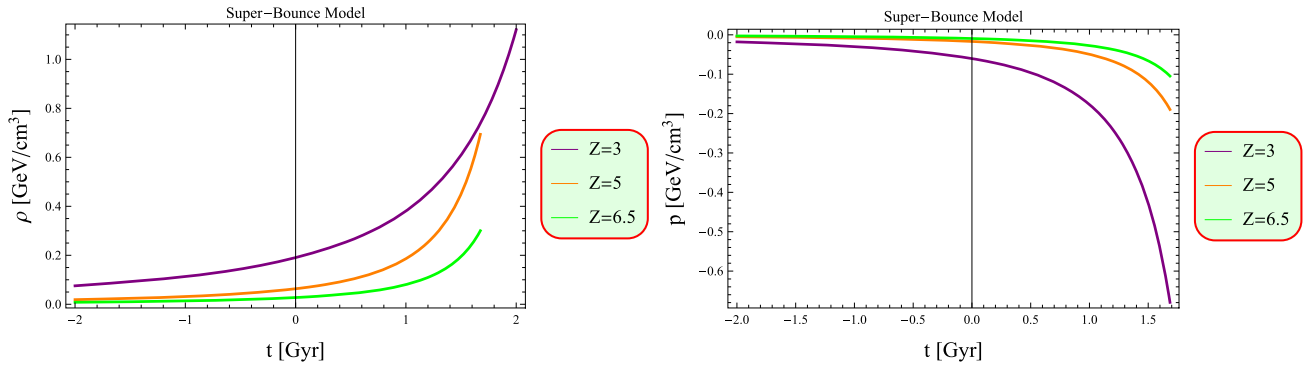

Fig. 5 Behavior of matter components versus cosmic time

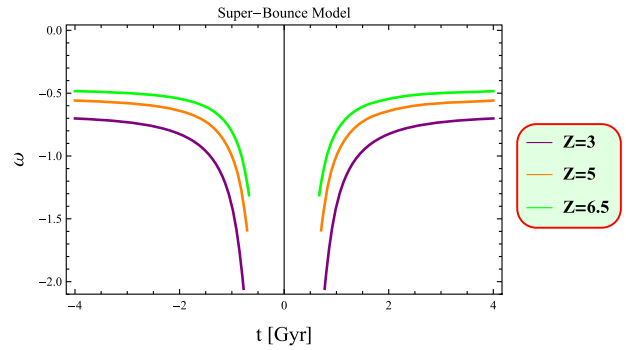

Fig. 6 Behavior of EoS parameter corresponding to cosmic time

in oscillatory-bounce model. The oscillatory-bounce model indicates that the cosmos undergoes a periodic cycles of contraction and expansion. This model shows that there are two distinct types of bounce events. The first type occurs when $t = \frac{n\pi t_\star}{\mathbb{B}}$, where n is an integer. This scenario corresponds to a big bang singularity marking a point where the cosmos contracts to a singular point before expanding again. The second type of bounce takes place when $t = \frac{(2n+1)\pi t_\star}{2\mathbb{B}}$. This occurs when the cosmos reaches its maximum size as expansion ends and the cosmos begins to contract again. This transitional behavior of cosmos is critical in understanding the dynamics of its evolution as predicted by this model.

The expressions for H and Q corresponding to this bouncing model turn out to be

$$H = \frac{2\mathbb{B}}{t_\star}\cot\left(\frac{\mathbb{B}t}{t_\star}\right), \quad Q = -\frac{24\mathbb{B}^2}{t_\star^2}\cot^2\left(\frac{\mathbb{B}t}{t_\star}\right). \tag{26}$$

The graphical behavior of the Hubble parameter in the oscillatory-bounce is shown in the right side of Fig. 7. The Hubble parameter becomes singular at bouncing point for $t = \frac{n\pi t_\star}{\mathbb{B}}$. Moreover, the Hubble parameter undergoes a transition phase of contraction and expansion at $t = \frac{(2n+1)\pi t_\star}{2\mathbb{B}}$. Specifically, it shifts from positive values to negative values at these points. This indicates that there is a critical moment, where the Hubble parameter crosses zero by changing its phase from expansion towards contraction.

Using Eq. (26) in Eqs. (13)–(14), we obtain the field equations corresponding to this model as

$$\rho = \frac{1}{t_\star^2(2\xi_2^2-49)}\Bigg[2\mathbb{B}^2\xi_1\Bigg(-6(\xi_2-7)\Bigg(\cot^2\left(\frac{\mathbb{B}t}{t_\star}\right)-2\Bigg) +(84-13\xi_2)\times\csc^2\left(\frac{\mathbb{B}t}{t_\star}\right)\Bigg)\Bigg], \tag{27}$$

$$p = \frac{1}{t_\star^2(2\xi_2^2-49)}\Bigg[2\mathbb{B}^2\xi_1\Bigg(-6(\xi_2-7)\Bigg(\cot^2\left(\frac{\mathbb{B}t}{t_\star}\right)-2\Bigg) +(70-9\xi_2)\times\csc^2\left(\frac{\mathbb{B}t}{t_\star}\right)\Bigg)\Bigg]. \tag{28}$$

Figure 8 depicts the change in matter variables for oscillatory-bounce model. This model demonstrates an oscillation in the behavior of the fluid parameters. Prior to the bounce, there is a positive increase in energy density and it displays a positive decrease after the bounce. Similarly, pressure exhibits a negative pattern in the behavior. These graphical behavior support the current cosmic expansion. Using Eqs. (27) and (28), we obtain the corresponding EoS parameter as

$$\omega = -\frac{6(\xi_2+7)\left(\cot^2\left(\frac{\mathbb{B}t}{t_\star}\right)-2\right)+(9\xi_2+70)\csc^2\left(\frac{\mathbb{B}t}{t_\star}\right)}{6(\xi 2-7)\left(\cot^2\left(\frac{\mathbb{B}t}{t_\star}\right)-2\right)+(13\xi 2-84)\csc^2\left(\frac{\mathbb{B}t}{t_\star}\right)} \tag{29}$$

Figure 9 shows that the EoS parameter oscillates over time reflecting the dynamic nature of the cosmological evolution under this framework. The graphical representation provides a powerful insight into the underlying physical processes driving the oscillations and their impact on the behavior of model.

3.4 Study of matter-bounce model

The matter-bounce scenario is a cosmological model proposed as an alternative to the big bang theory. In the matter-

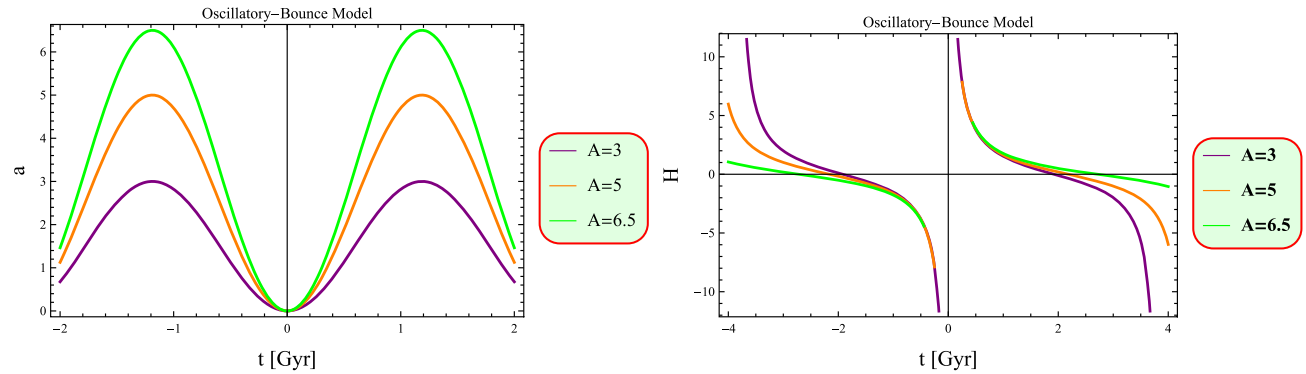

Fig. 7 Behavior of scale factor and Hubble parameter versus cosmic time

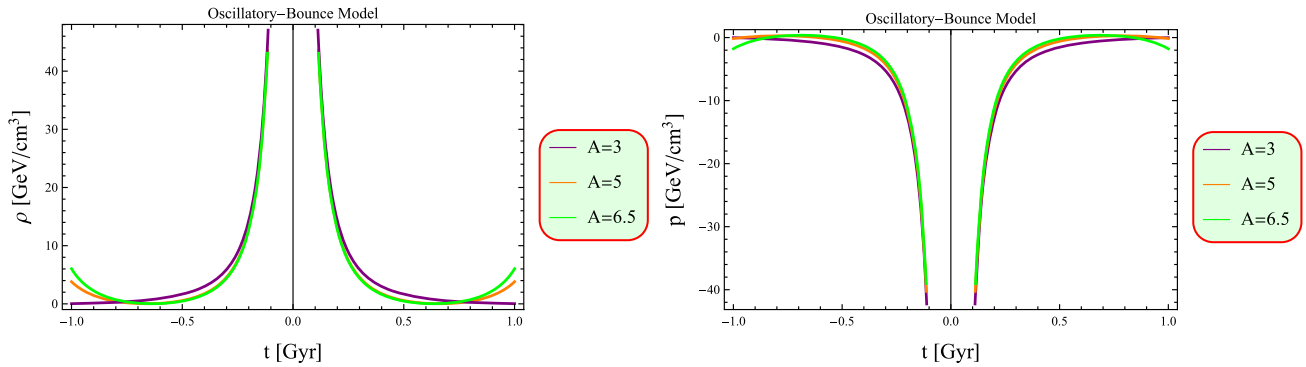

Fig. 8 Behavior of energy density and pressure for different values of $\mathbb{A}$

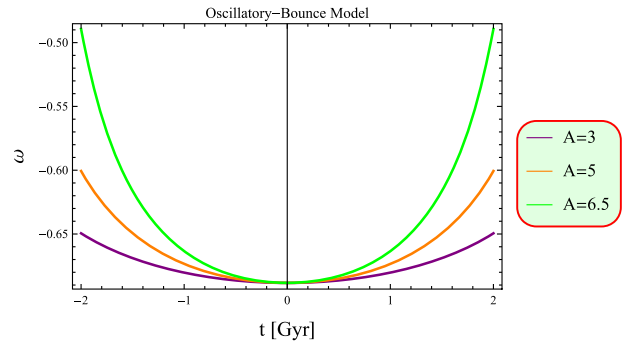

Fig. 9 Behavior of EoS parameter for different values of $\mathbb{A}$

bounce model, the cosmos undergoes a phase of contraction before expanding again, rather than beginning from a singularity as in the big bang theory. The motivation for the matter-bounce model arises from addressing some of the theoretical issues present in the standard big bang model. The matter-bounce model attempts to provide an alternative framework that avoids initial singularities. An intriguing method alternative to inflation is the concept of matter-bounce model [59], which is notable for its compatibility with observational evidence from the Planck observational data [60]. The corresponding scale factor is expressed as

$$a = \mathbb{A}\left(\frac{3}{2}\rho_c t^2 + 1\right)^{\frac{1}{3}}. \tag{30}$$

In the given context, $0 < \rho_c < 1$ represents a critical density. The critical density is a fundamental concept in cosmology used to understand the fate and geometry of the cosmos based on its overall density. In the left plot of Fig. 10 demonstrates the behavior of matter-bounce scale factor is positive and symmetric on either side of the bouncing point. The Hubble parameter and non-metricity scalar for this case are given by

$$H = \frac{2t\rho_c}{2 + 3\rho_c t^2}, \quad Q = -6\left(\frac{2t\rho_c}{2 + 3\rho_c t^2}\right)^2. \tag{31}$$

In the right side of Fig. 10 illustrates the behavior of the Hubble parameter across different phases of the cosmic bounce. In the pre-bounce phase, the Hubble parameter is negative, indicating a contracting universe. As the cosmos approaches towards the critical bounce point, the Hubble parameter reaches to zero which signifies a momentary end in the contraction and marking the transition between contraction and expansion phases. By following the bouncing point during the post-bounce epoch, the Hubble parameter becomes positive reflecting the cosmic expansion. This tran-

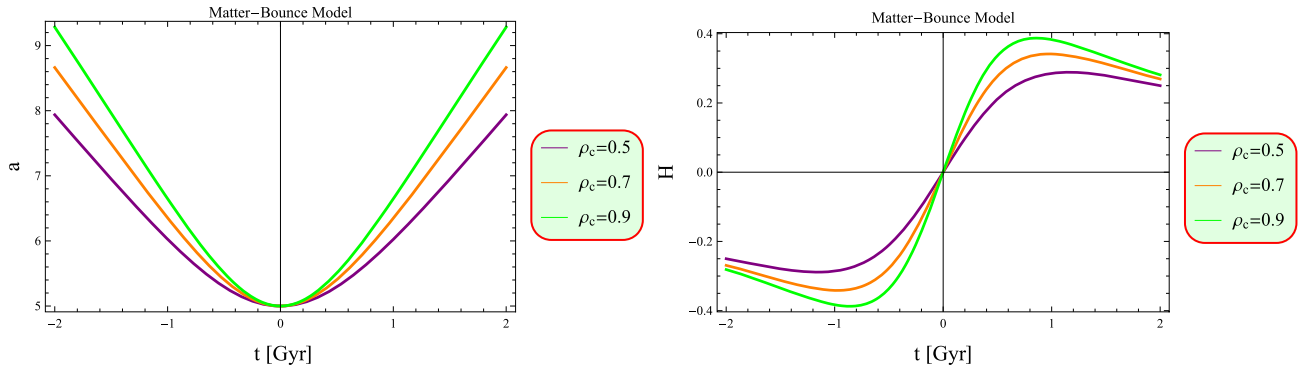

Fig. 10 Behavior of scale factor and Hubble parameter to cosmic time

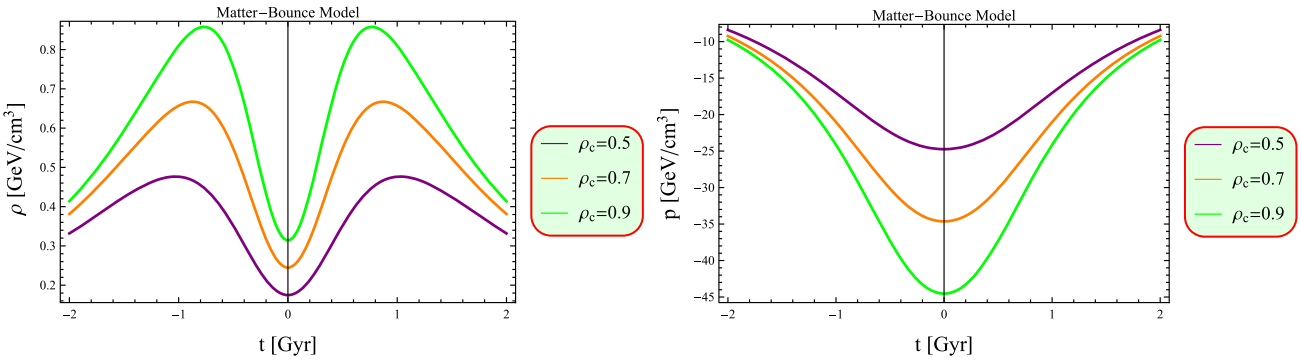

Fig. 11 Behavior of energy density and pressure for different values of ρ_c

sition through the phases highlight the dynamic nature of the cosmological model. Substituting Eq. (31) into Eqs. (13)–(14), the resulting field equations are expressed as

$$\rho = \frac{1}{(2\xi_2\rho_c^2 - 49)(3t^2\rho_c + 2)^2} \left[2\xi_1\rho_c(2\xi_2 - 21t^2\rho_c(\xi_2 - 6))\right], \tag{32}$$

$$p = \frac{1}{(2\xi_2\rho_c^2 - 49)(3t^2\rho_c + 2)^2} \left[2\xi_1\rho_c(28 + 84t^2\rho_c + \xi_2(9t^2\rho_c + 6))\right]. \tag{33}$$

Figure 11 determines that the behavior of fluid parameters is consistent with the expected behavior of DE model. Using Eqs. (32) and (33), the EoS parameter for this bouncing model is as follows

$$\omega = -\frac{28 + 6\xi_2 + 3t^2(28 + 3\xi_2)\rho_c}{-2\xi_2 + 21t^2(\xi_2 - 6)\rho_c}. \tag{34}$$

Figure 12 demonstrates that the EoS parameter becomes singular at the bouncing point and undergoes rapid changes near the bounce. Notably, the EoS parameter shows symmetry around the bouncing epoch and exhibits significant evolution in the phantom region. This evolution describes the dynamical change in the nature of matter and energy in the cosmos during this critical phase.

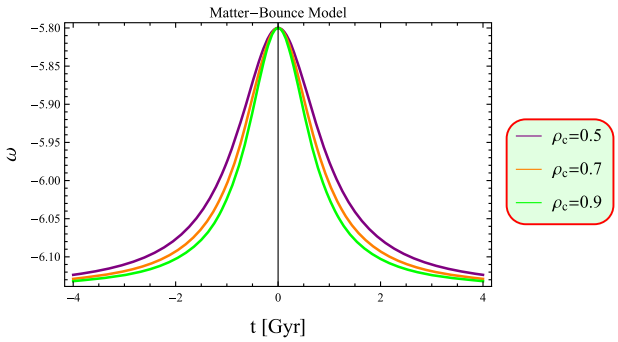

Fig. 12 Behavior of EoS parameter for different values of ρ_c

3.5 Discussion on exponential-bounce model II

The exponential model describes the expansion history of the cosmos. This model is an extension of the original exponential model (also known as the exponential inflationary universe or exponential expansion) to explain the rapid expansion of the universe in the early moments of the big bang. In the context of theories related to inflation and the dynamics of the cosmic expansion, this model is referred to a bouncing scenario where the scale factor evolves exponentially with time. In this bouncing model, the scale factor is represented

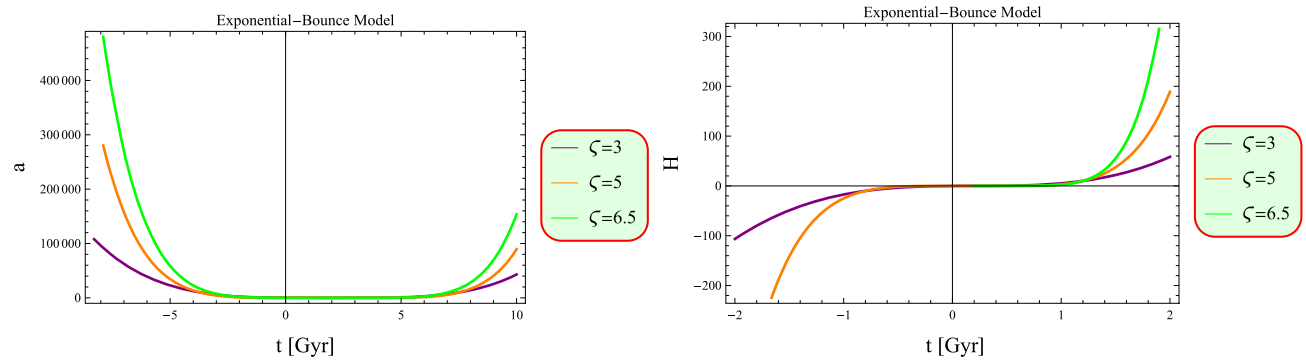

Fig. 13 Behavior of scale factor and Hubble parameter to cosmic time

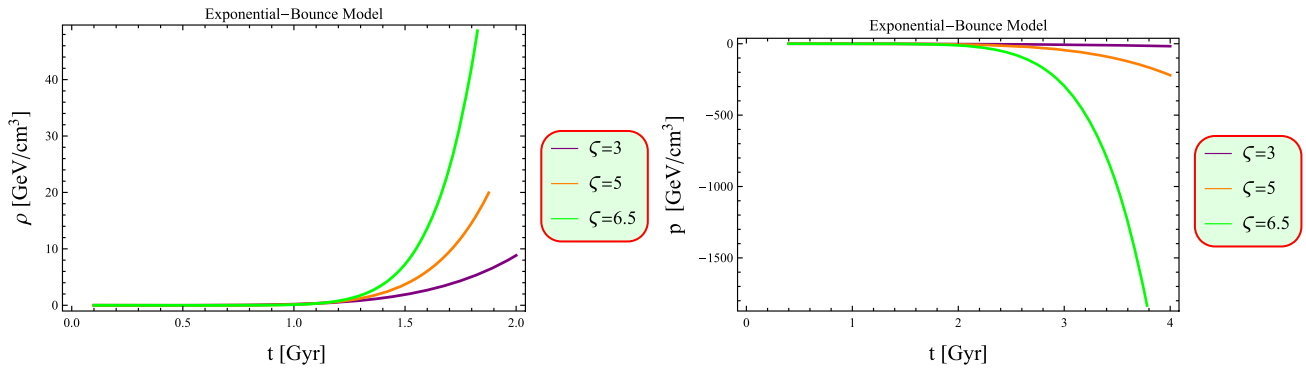

Fig. 14 Behavior of energy density and pressure for different values of ς

as

$$a = \mathbb{A}\left(\frac{h_0}{\varsigma+1}(t-t_b)^{\varsigma+1}\right), \tag{35}$$

where h_0 and ς are an arbitrary constant. The graphical representation of scale factor is shown in the left plot of Fig. 13 for different values of model parameter (ς). The graph indicates positive and an asymmetrical pattern in the behavior of the scale factor relative to time in the exponential-bounce model II.

The corresponding Hubble parameter and non-metricity are given as follows

$$H = h_0(t-t_b)^{\varsigma}, \quad Q = -6h_0^2(t-t_b)^{2\varsigma}. \tag{36}$$

The right plot of Fig. 13 demonstrates that the Hubble parameter becomes singular at bouncing point and this specific value denotes the location of the bounce. Prior to the bounce, the Hubble parameter is negative and becomes positive in the post-bounce phase. This change signifies the transition from a contracting to an expanding phases in the cosmic evolution. By applying Eq. (36) in Eqs. (13)–(14), we obtain

$$\rho = \frac{1}{(2\xi_2^2-49)}\big[h_0(t-t_b)^{\varsigma-1}\xi_1(-9h_0(t-t_b)^{\varsigma-1})(\xi_2-7) + \varsigma\xi_2\big], \tag{37}$$

$$p = \frac{1}{(2\xi_2^2-49)}\big[h_0(t-t_b)^{\varsigma-1}\xi_1(9h_0(t-t_b)^{\varsigma-1})(\xi_2+7) + \varsigma(3\xi_2+14)\big]. \tag{38}$$

In Fig. 14, the energy density shows an upward trend whereas the pressure demonstrates a downward pattern, aligning with the anticipated behavior in the DE model. Using Eqs. (37) and (38), we get

$$\omega = \frac{(9h_0(t-t_b)^{\varsigma+1})(\xi_2+7)+\varsigma(3\xi_2+14)}{(-9h_0(t-t_b)^{\varsigma+1})(\xi_2-7)+\varsigma\xi_2)} \tag{39}$$

The EoS parameter does not display symmetry around the bouncing epoch and evolves in the phantom region as shown in Fig. 15. In the context of $f(Q,T)$ gravity, this exponential-bounce model II demonstrates behavior similar to the exponential model I.

4 Analysis of different physical aspects

In this section, we explore a comprehensive analysis of various physical aspects like deceleration parameter, energy conditions and redshift analysis that influence the study of different cosmological solutions. By examining the behavior of

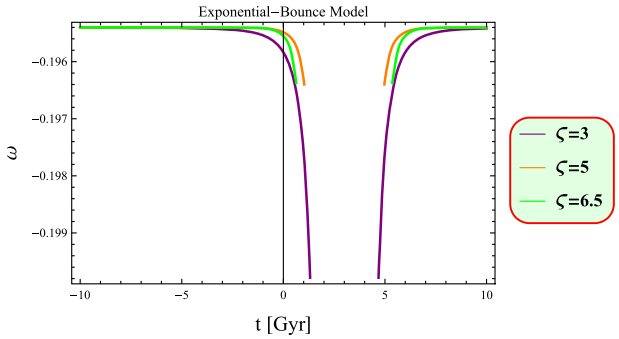

Fig. 15 Behavior of EoS parameter for different values of ς

these parameters, we aim to uncover insights that contribute to a deeper understanding of cosmic dynamics.

4.1 Deceleration parameter

The deceleration parameter (q) is a dimensionless quantity which measures the rate of expansion of the universe. It is defined as

$$q = -\frac{a\dot{a}}{\dot{a}^2} = -1 - \frac{\dot{H}}{H^2}. \tag{40}$$

The positive value of deceleration parameter indicates an decelerated cosmos whereas a negative value demonstrates an accelerated universe. The asymmetrical nature of the deceleration parameter is shown in the Fig. 16. The negative value of deceleration parameter indicates that the universe is undergoing accelerated expansion. This behavior aligns with observations of distant supernova and the cosmic microwave background, which provide evidence for the influence of dark energy driving the accelerated expansion.

4.2 Analysis of energy conditions

Energy conditions are viable constraints with specific physical properties based on the energy-momentum tensor used to assess the physical consistency of cosmic models. Researchers impose these constraints to evaluate the viability of different cosmic configurations. The energy bounds are classified into several types as null energy condition $(0 \leq \rho + p)$, dominant energy condition $(0 \leq \rho, 0 \leq \rho \pm p)$, weak energy condition and strong energy condition $(0 \leq \rho + p, 0 \leq \rho + 3p)$. In this study, we present a graphical representation of these energy constraints for all considered bouncing cosmological models. By examining these conditions, we can understand the characteristics of cosmic geometries and their relationship to the EMT. The violation of the null energy condition implies the violation of all other energy conditions, which guarantees the existence of a non-singular bounce [61].

Figures 17, 18, 19, 20 and 21 demonstrate that the bouncing criteria of the cosmos is satisfied for all the considered models, providing a comprehensive analysis of these conditions under which the universe exhibit a bounce epoch, ensuring the avoidance of singularities. The detailed graphical representation supports the stability and consistency of non-singular bounce in this theoretical framework. These results underscore the interplay between energy condition violations and the bouncing behavior. The violation of energy conditions is a critical requirement for the realization of a non-singular bounce.

4.3 Evaluation of redshift

In this section, we examine the redshift parameter (z) to study the behavior of matter configuration and cosmological scenario. The scale factor is given by $a(t) = a_0 t^{\varphi}$, where φ is an arbitrary constant and we assume the current value of a_0 as 1. The value of deceleration parameter is used as defined in Eq. (40). By using the value of $\varphi = \frac{1}{1+q}$ in scale factor, we have

$$a(t) = t^{\frac{1}{1+q}}, \tag{41}$$

where $q = -0.831^{+0.091}_{-0.091}$ [62]. The rate at which the universe is currently expanding can be described as

$$H = \frac{\dot{a}}{a} = H = (1+q)^{-1} t^{-1}, \quad H_0 = (1+q)^{-1} t_0^{-1}. \tag{42}$$

The expansion of the universe is affected by parameters such as q and H_0. To analyze the connection between the redshift parameter and the scale factor, we have

$$H = H_0(1+z)^{1+q}, \quad \dot{H} = -H_0(1+z)^{2+2q}. \tag{43}$$

The value of non-metricity in Eq. (11) is determined as

$$Q = -6H_0^2(1+z)^{2+2q}. \tag{44}$$

The field equations in terms of redshift are given by

$$\rho = \frac{-1}{49 + 2(\xi_2 - 7)\xi_2}[9\xi_1(\xi_2 - 7)H_0^2(z+1)^{2q+2}], \tag{45}$$

$$p = \frac{1}{(49 + 2(\xi_2^2 - 7)\xi_2}[9\xi_1(\xi_2 - 7)H_0^2(z+1)^{2q+2}]. \tag{46}$$

Figure 22 shows the variation of energy density and pressure as function of redshift for the considered $f(Q,T)$ model. The graphical behavior shows that the energy density increases and remains positive while the pressure decreases negatively which is consistent with the behavior of the DE. The EoS parameter is essential in cosmology because it describes the relationship between the pressure and density of the cosmic matter. Figure 23 demonstrates the graphical behavior of the EoS parameter as a function of redshift. This parameter shows the phantom region $(\omega < -1)$ which indicates an accelerated expansion of the universe.

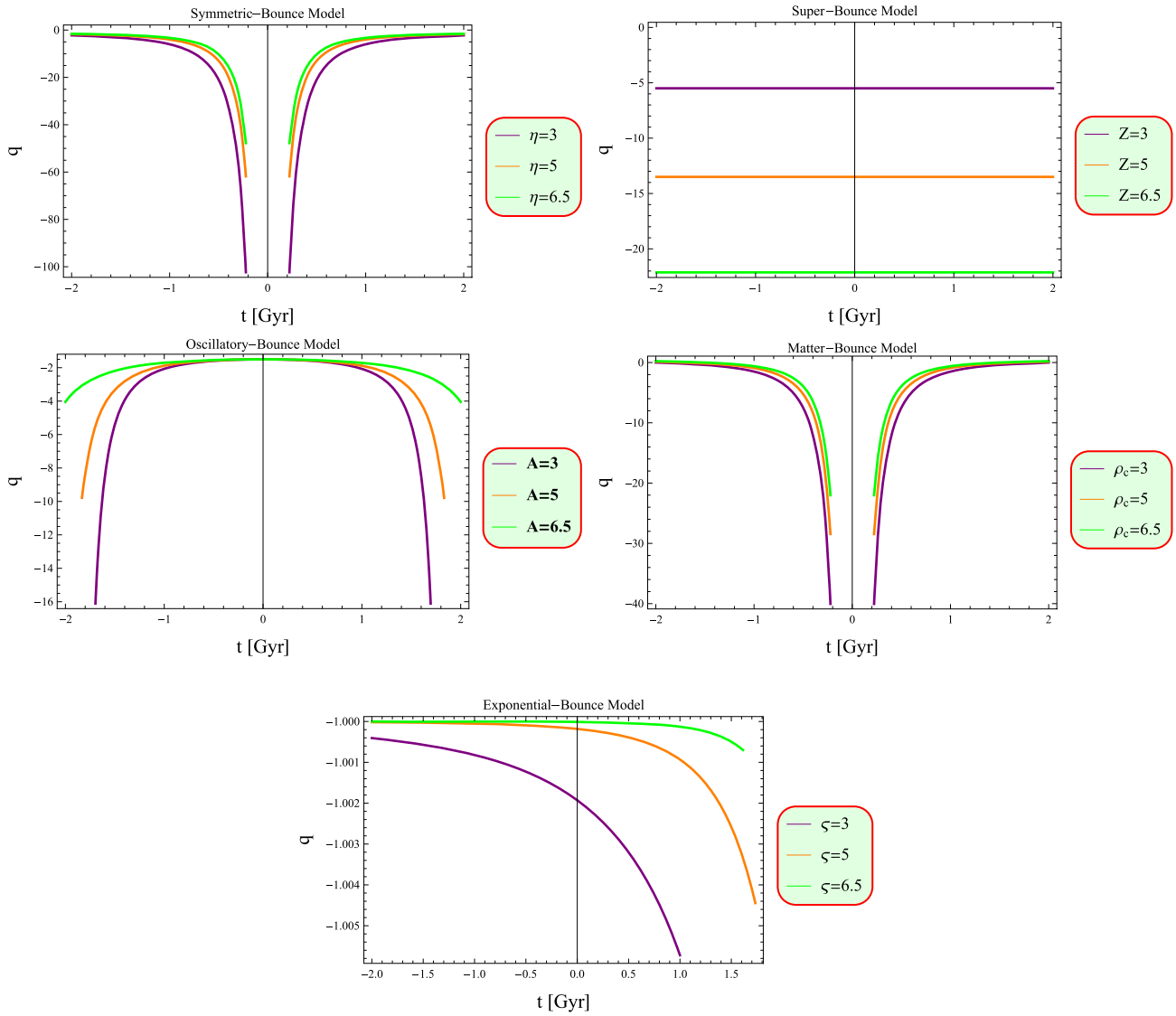

Fig. 16 Behavior of deceleration parameter for all the bouncing models

5 Final remarks

Recent cosmological observations, including measurements of cosmic microwave background radiation, Planck data, supernovae type-Ia, large-scale structures and galaxy redshift surveys indicate that the expansion of the cosmos is accelerating [63–66]. This discovery has led to the paradigm of modified theories of gravity as a fundamental framework for understanding gravitational interactions and their influence on cosmic expansion. These modified theories incorporate additional gravitational fields, spatial dimensions and higher-order derivatives offering diverse approaches to explain the phenomenon of cosmic acceleration through modifications to EGTR. The big bang cosmology faces significant challenges with the initial singularity and inflationary paradigm prompting diverse solutions in the literature. Several methods have been employed in the literature to address this issue and bouncing cosmology is considered as one of the most effective alternatives. Additionally, modified gravity offers a promising framework for developing new cosmological models that can eliminate the long-standing cosmological challenges. This study aims to investigate the singularity issue in the context of $f(Q,T)$ gravity using bouncing cosmology.

The motivation to investigate the bouncing cosmology in the framework of $f(Q,T)$ theory is to examine the viability of non-singular bouncing solutions. By using different constraints, it is possible to assess the validity of this theory in comparison to other cosmic models. Therefore, integrating bouncing cosmology in the modified $f(Q,T)$ theory offers

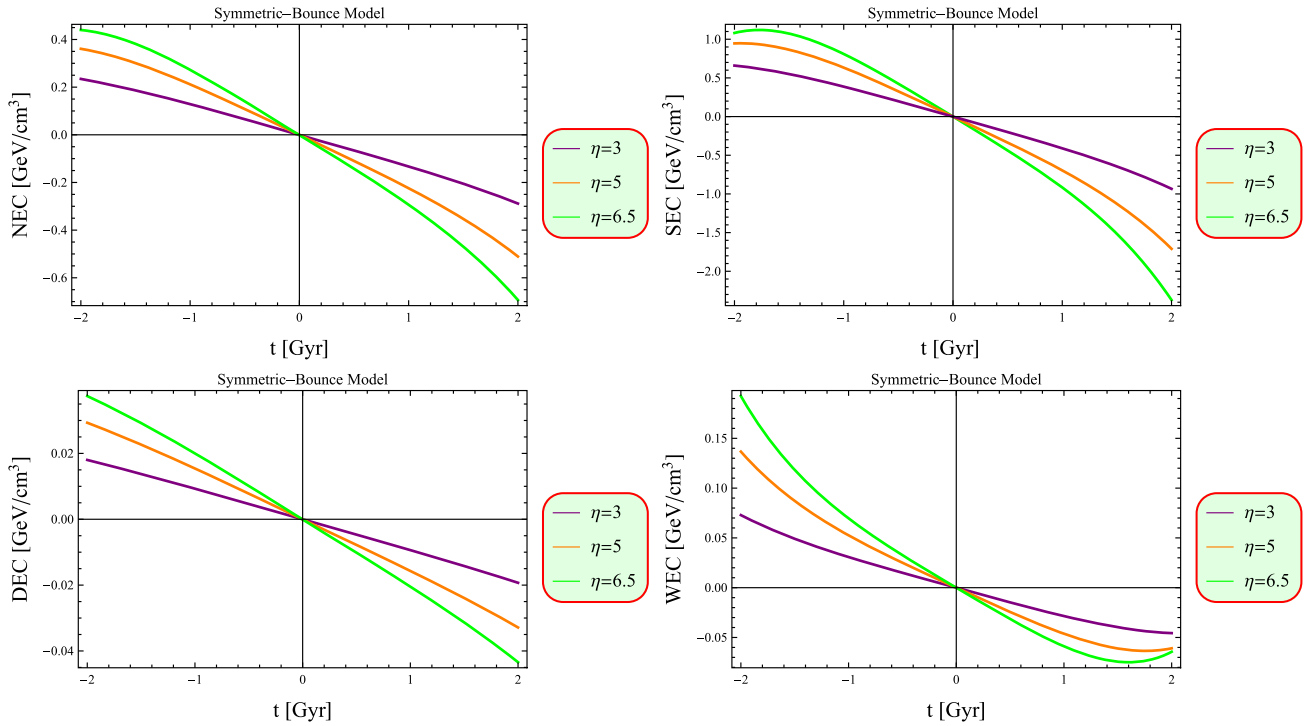

Fig. 17 Behavior of energy conditions for different parametric values

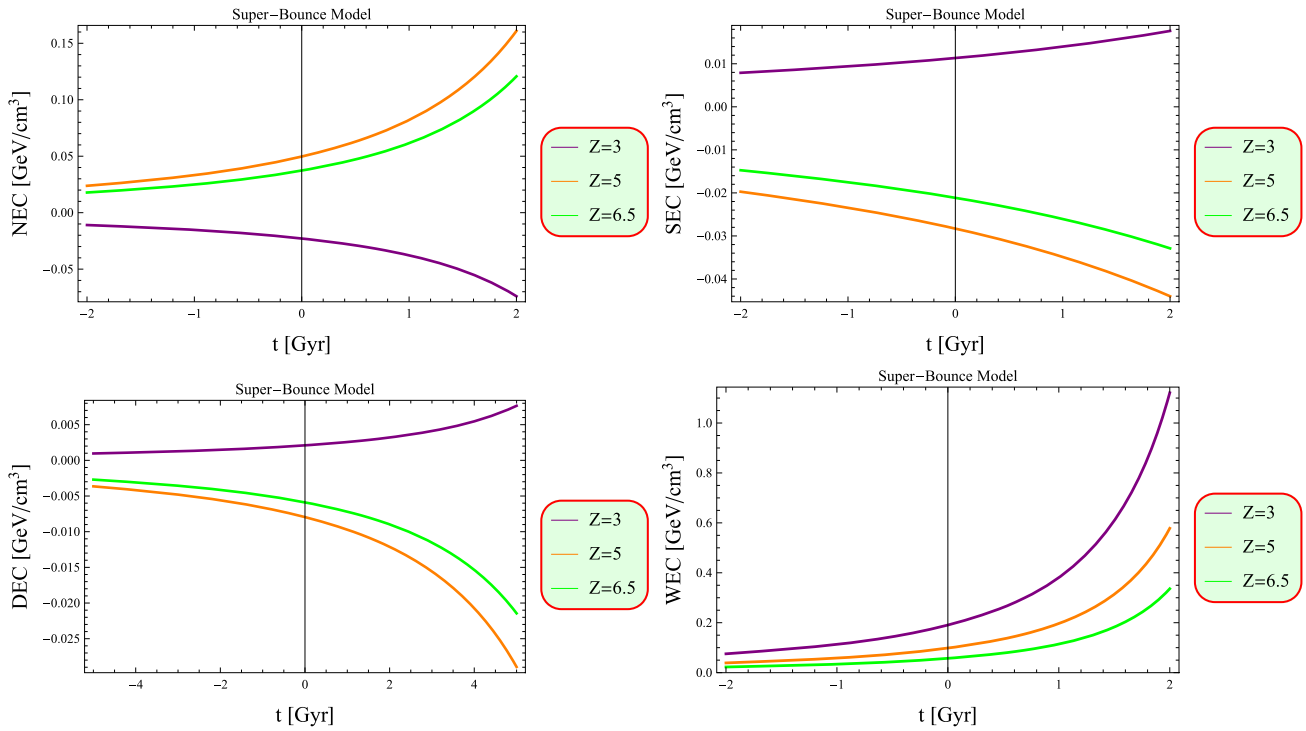

Fig. 18 Analysis of energy conditions corresponding to cosmic time

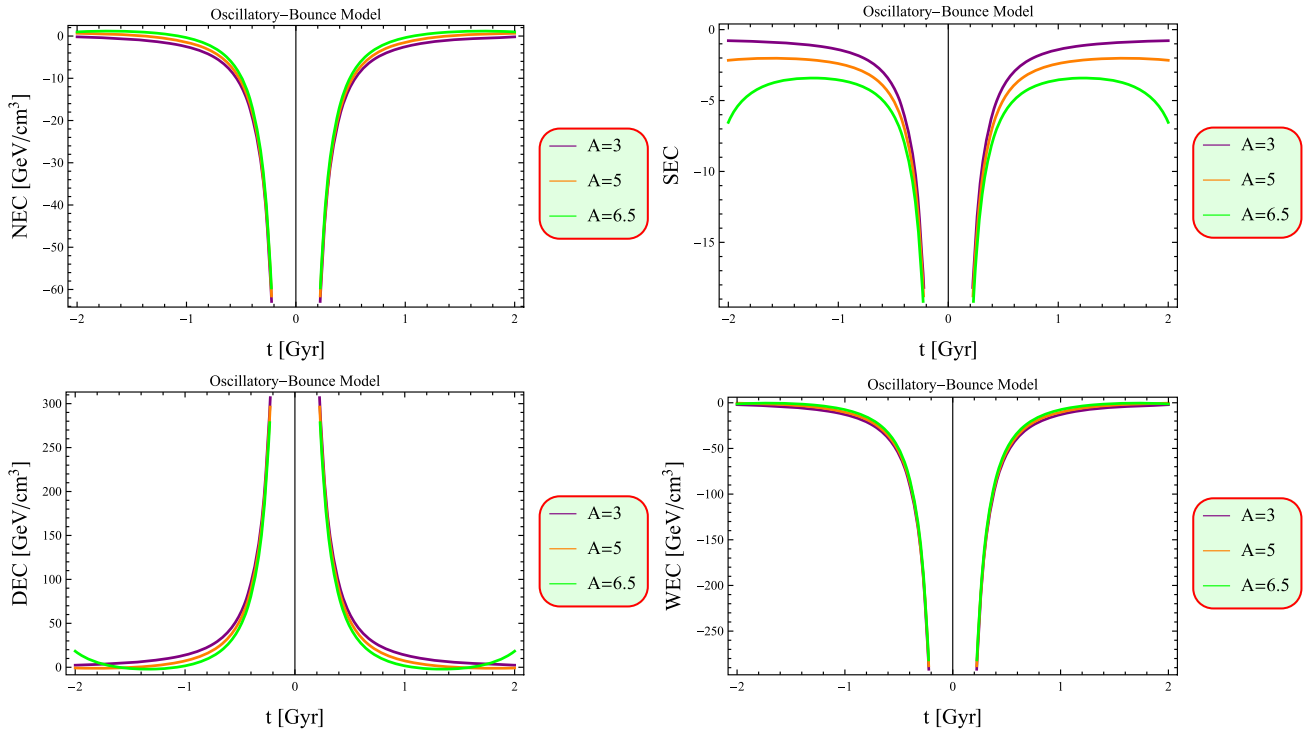

Fig. 19 Graphs of energy constraints for oscillatory-bounce model

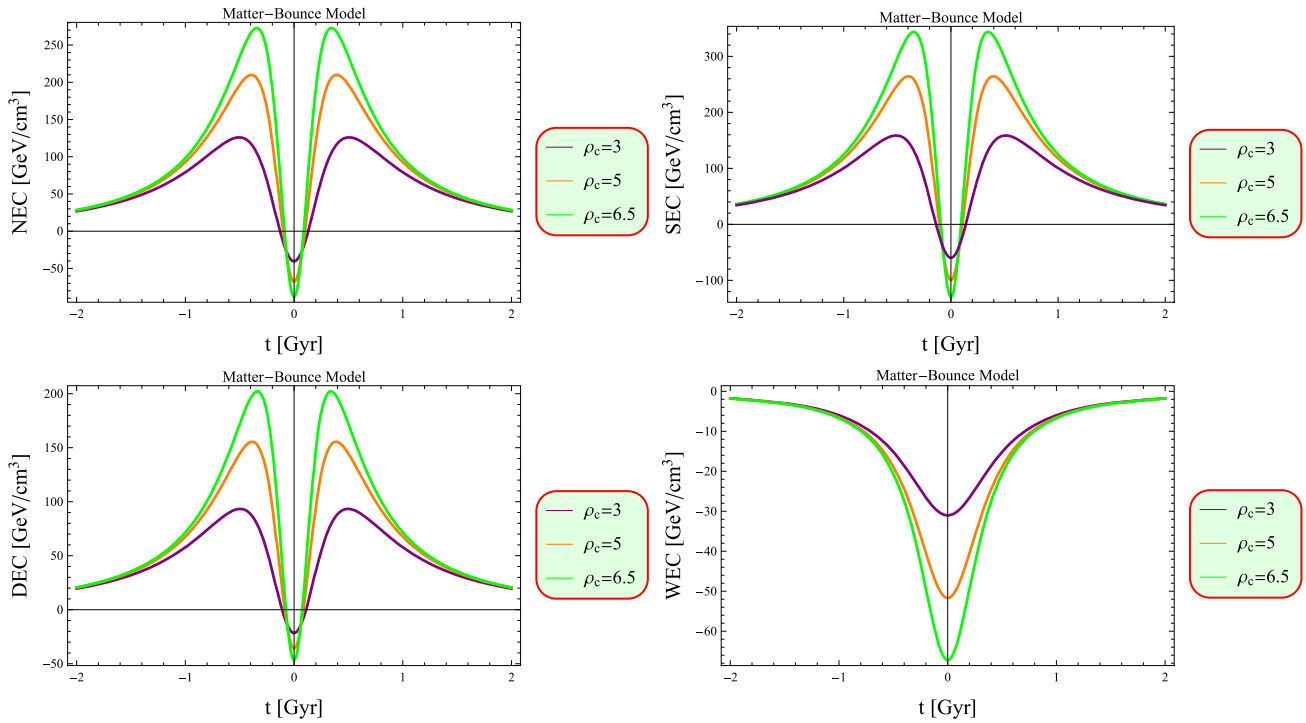

Fig. 20 Evaluation of energy conditions for different values of ρ_c

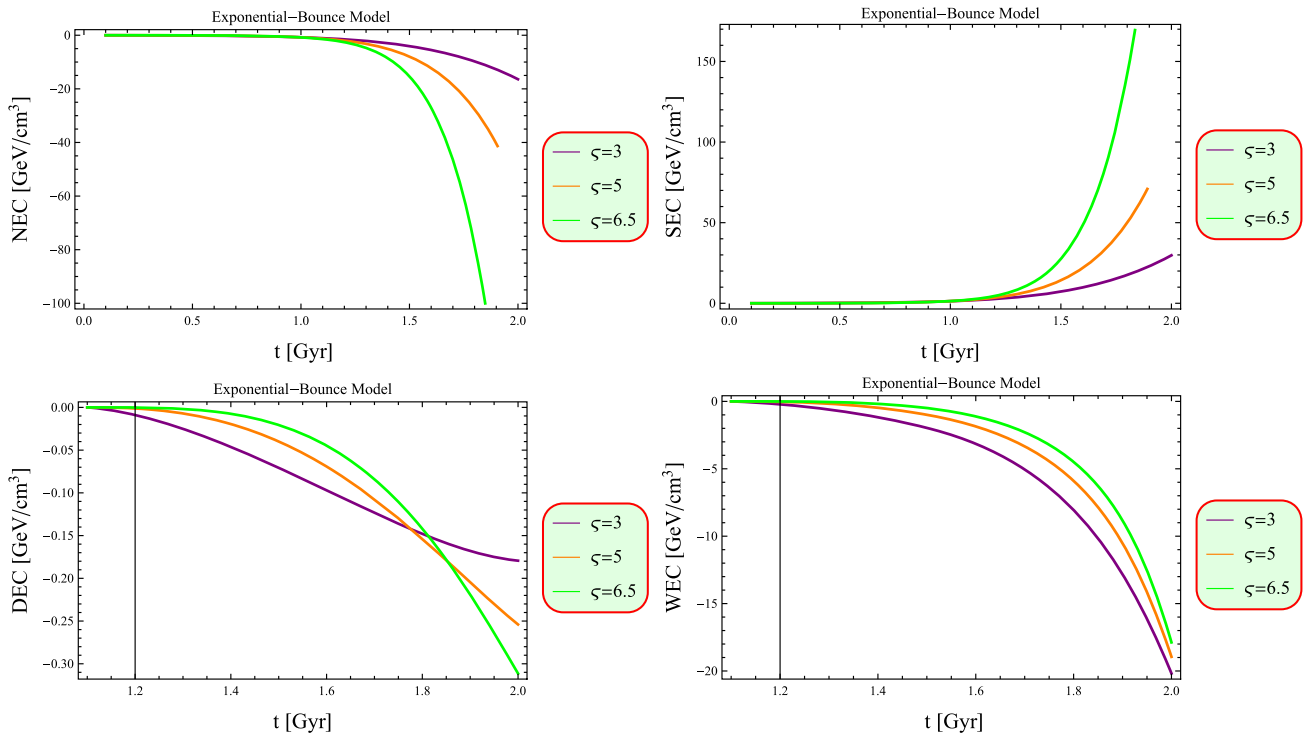

Fig. 21 Behavior of energy bounds for exponential-bounce model

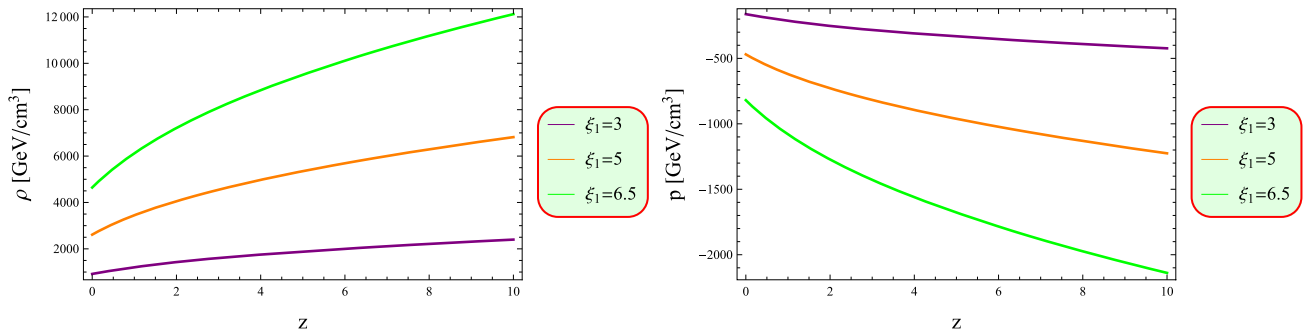

Fig. 22 Behavior of matter variables corresponding to redshift

a platform to address the fundamental inquiries in cosmology such as the cosmic origin, DE/dark matter nature and behavior of gravity at classic and quantum levels. The main goal of this research is to examine how $f(Q, T)$ gravity contributes to construct effective cosmological models which explore the issue of accelerated expansion of the cosmos and its potential implications. The rate of cosmic expansion is determined by using different scale factors and the Hubble parameters. There are two scenarios to consider, i.e., the scale factor approaches to zero (big bang singularity) or considering the bouncing models. In the cosmic bounce models, the scale factor never reaches to zero, thus avoiding any spacetime singularity. Initially, the cosmos expands, then contracts and this cycle of expansion and contraction continues until to reach a minimum size of the scale factor.

We have focused on investigating the familiar bouncing cosmological scenarios in a flat FRW spacetime characterized by a perfect fluid matter distribution. Our study encompasses five distinct types of bouncing solutions, including symmetric-bounce, super-bounce, oscillatory-bounce, matter-bounce, and exponential bouncing models. We have analyzed the cosmological parameters including scale factor, Hubble parameter, EoS parameter, deceleration parameter and behavior of energy conditions associated with each of these solutions. The main findings are summarized as follows.

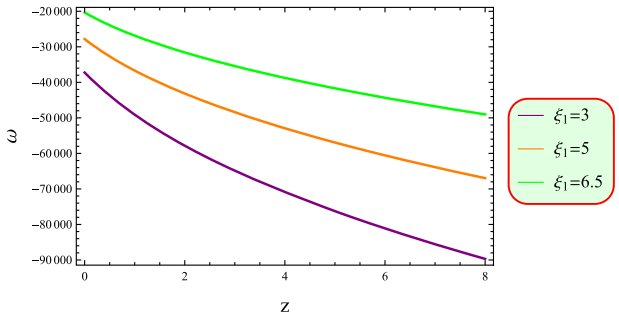

Fig. 23 Behavior of EoS parameter versus redshift

- The scale factor is a positive function that varies over time to describe the changing size of the cosmos, reflecting its expansion dynamics with respect to cosmic time (left plot of Figs. 1, 4, 7, 10 and 13). These graphs exhibit a symmetrical pattern illustrating that these scale factors increase and decrease evenly on both sides of a bouncing point except exponential model II scale factor.
- The Hubble parameter is negative during the pre-bounce phase indicating a contracting cosmos. As the universe approaches the critical bouncing point ($t = 0$), the Hubble parameter approaches to zero. Moving into the post-bounce epoch, the Hubble parameter becomes positive which signifies the cosmic expansion. This progression through the phases describes the dynamic nature of all the considered cosmic model as it transitions between contraction and expansion phases.
- The graphical behavior of energy density and pressure reveals a an inverse relationship between energy density and pressure which is in accordance with the expected behavior predicted by the DE model.
- The EoS parameter helps us to comprehend how different energy components interact and influence the overall dynamics during the bouncing point. At the point of bounce, the EoS parameter becomes singular and undergoes rapid change. It shows symmetry around the bounce epoch and transitions into the phantom region. This change signifies a significant shift in the characteristics of this parameter as it moves towards the bouncing point.
- The behavior of deceleration parameter is crucial to understand the cosmic dynamics. The deceleration parameter shows the cosmic accelerated expansion as shown in Fig. 16. This behavior is consistent with the cosmological observations and also describes the role of dark energy in driving this accelerated expansion.
- We have discussed the cosmic acceleration and expansion through energy conditions in this framework. The NEC is violated for all the bouncing models which ensures the existence of non-singular cosmic bounce in this modified framework (Figs. 17, 18, 19, 20, 21).
- The energy density in terms of redshift function shows positively increasing behavior while pressure demonstrates the negatively decreasing behavior for the considered $f(Q, T)$ model, confirming that the cosmos is in the expansion phase (Fig. 22).
- The graphical behavior of the EoS parameter corresponding to redshift represents the phantom region, which shows the cosmic accelerated expansion (Fig. 23).

We have examined the existence of non-singular cosmic bounce models under the influence of modified $f(Q, T)$ terms. Our analysis on the physical aspects has unveiled a feasible profile of cosmological models. We have investigated several fundamental bounce models including symmetric-bounce, super-bounce, oscillatory-bounce, matter-bounce and exponential-bounce that delineate the cosmic evolution. It is worth noting that all these models indicate the presence of viable bouncing cosmology in this theoretical framework. In a recent paper, Gadbail et al. [67] investigated various cosmic bounce models in $f(Q)$ gravity and explored cosmic evolution using fixed parametric values. Agrawal and his colleagues [68] studied the matter-bounce scenario in $f(R, T)$ theory for various parametric values greater than 1. We have done graphical analysis for both values less and greater than 1. Our findings not only coincide with the existing literature but also provide further understanding of the dynamics of cosmic evolution. Our results demonstrate that cosmic solutions remain feasible even when considering modified terms, highlighting the strength of our theoretical framework.

Data Availability Statement My manuscript has no associated data. [Authors' comment: Data sharing not applicable to this article as no datasets were generated or analysed during the current study.]

Code Availability Statement My manuscript has no associated code/software. [Authors' comment: Code/Software sharing not applicable to this article as no code/software was generated or analysed during the current study].

Funded by SCOAP[3].

References

1. H. Weyl, Sitzungsber. Preuss. Akad. Wiss. **2**(6), 465 (1918)
2. P.A.M. Dirac, Proc. R. Soc. A Math. Phys. Eng. Sci. **333**, 403 (1973)
3. M. Novello, S.P. Bergliaffa, Phys. Rep. **463**, 127 (2008)
4. J.B. Jimenez, L. Heisenberg, T. Koivisto, Phys. Rev. D **9**(8), 044048 (2018)
5. A.D. Felice, S.R. Tsujikawa, Living Rev. Relativ. **1**(3), 3 (2010)
6. T. Harko et al., Phys. Rev. D **8**(4), 024020 (2011)
7. M. Sharif, M.Z. Gul, Eur. Phys. J. Plus **133**, 345 (2018)
8. M. Sharif, M.Z. Gul, Mod. Phys. Lett. A **3**(6), 2150214 (2021)
9. M. Sharif, M.Z. Gul, Ann. Phys. **465**, 169674 (2024)
10. M. Sharif, M.Z. Gul, Phys. Scr. **9**(9), 065036 (2024)
11. M.Z. Gul, M. Sharif, I. Hashim, Phys. Dark Univ. **4**(5), 101537 (2024)
12. M.Z. Gul, M. Sharif, Phys. Scr. **9**(9), 055036 (2024)
13. M.Z. Gul, M. Sharif, Chin. J. Phys. **8**(8), 388 (2024)
14. M.Z. Gul, M. Sharif, New Astron. **106**, 102137 (2024)
15. Y. Xu et al., Eur. Phys. J. C **7**(9), 708 (2019)
16. S. Arora et al., Phys. Dark Univ. **3**, 100664 (2020)
17. S. Arora, J.R.L. Santos, P.K. Sahoo, Phys. Dark Univ. **3**(1), 100790 (2021)
18. M. Adeel et al., Mod. Phys. Lett. A **3**(8), 2350152 (2023)
19. S. Rani et al., Int. J. Geom. Methods Mod. Phys. **2**(1), 2450033 (2024)
20. M.Z. Gul et al., Eur. Phys. J. C **8**(4), 8 (2024)
21. M.Z. Gul, M. Sharif, A. Arooj, Fortschr. Phys. **7**(2), 2300221 (2024)
22. M.Z. Gul, M. Sharif, A. Arooj, Phys. Scr. **9**(9), 045006 (2024)
23. M.Z. Gul, M. Sharif, A. Arooj, Gen. Relativ. Gravit. **5**(6), 45 (2024)
24. G.P. Singh, A.R. Lalke, Indian J. Phys. **9**(6), 4361 (2022)
25. Y. Xu et al., Eur. Phys. J. C **8**(3), 400 (2023)
26. G.N. Gadbail, S. Arora, P.K. Sahoo, Phys. Lett. B **838**, 137710 (2023)
27. S.A. Narawade, M. Koussour, B. Mishra, Nucl. Phys. **992**, 116233 (2023)
28. K. Bourakadi et al., Phys. Dark Univ. **4**(1), 101246 (2023)
29. S.H. Shekh et al., J. High Energy Astrophys. **3**(9), 53 (2023)
30. M. Khurana et al., Phys. Dark Univ. **4**(3), 101408 (2024)
31. M. Sharif, I. Ibrar, Chin. J. Phys. **8**(9), 1578 (2024)
32. Y.F. Cai et al., J. High Energy Phys. **1**, 071 (2007)
33. Y.F. Cai, D.A. Easson, R. Brandenberger, J. Cosmol. Astropart. Phys. **08**, 020 (2012)
34. C. Li, R. Brandenberger, Y.K.E. Cheung, Phys. Rev. D **9**, 123535 (2014)
35. Y.F. Cai et al., J. Cosmol. Astropart. Phys. **1**, 024 (2013)
36. Bamba, K., Haro, J., Odintsov, S.D.: J. Cosmol. Astropart. Phys. **02**, 008 (2013)
37. M. Ilyas, W.U. Rahman, Eur. Phys. J. C **8**(1), 001 (2021)
38. M.F. Shamir, Phys. Dark Univ. **3**(2), 100794 (2021)
39. M. Sharif, M.Z. Gul, Phys. Scr. **9**(6), 105001 (2021)
40. M. Sharif, M.Z. Gul, Phys. Scr. **9**(6), 025002 (2021)
41. M. Sharif, M.Z. Gul, Phys. Scr. **9**(6), 125007 (2021)
42. M. Sharif, M.Z. Gul, Eur. Phys. J. Plus. **136**, 503 (2021)
43. M. Sharif, M.Z. Gul, Chin. J. Phys. **8**, 58 (2022)
44. M. Zubair, Q. Muneer, S. Waheed, Int. J. Mod. Phys. D. **3**(1), 2250092 (2022)
45. M. Zubair, M. Farooq, E. Gudekli, Int. J. Geom. Methods Mod. Phys. **1**(9), 2250135 (2022)
46. M.G. Ganiou et al., Eur. Phys. J. Plus **137**, 208 (2022)
47. J.K. Singh et al., J. High Energy Phys. **03**, 191 (2023)
48. M.J.S. Houndjo et al., Chin. J. Phys. **8**(3), 558 (2023)
49. M. Sharif, M.Z. Gul, N. Fatima, New Astron. **109**, 102211 (2024)
50. A.S. Agrawal et al., Phys. Dark Univ. **3**(3), 100863 (2021)
51. S. Capozziello, V.F. Cardone, A. Troisi, Phys. Rev. D **7**(1), 043503 (2005)
52. S. Nojiri, S.D. Odintsov, J. Phys. Conf. Ser. **6**(6), 012005 (2007)
53. Y.F. Cai, D.A. Easson, R. Brandenberger, J. Cosmol. Astropart. Phys. **08**, 020 (2012)
54. S. Nojiri, S.D. Odintsov, V.K. Oikonomou, Phys. Rev. D **9**(3), 084050 (2016)
55. K. Bamba et al., J. Cosmol. Astropart. Phys. **01**, 008 (2014)
56. M. Sharif, M. Ajmal, Chin. J. Phys. **8**(8), 706 (2024)
57. M. Koehn, J. Lehners, B.A. Ovrut, Phys. Rev. D **9**, 025005 (2014)
58. J. Khoury, P.J. Steinhardt, N. Turok, Phys. Rev. Lett. **9**(2), 031302 (2004)
59. J. Haro et al., Phys. Rev. D **9**(2), 124026 (2015)
60. P.A.R. Ade et al., Astron. Astrophys. **586**, 138 (2016)
61. E.A. Kontou, K. Sanders, Class. Quantum Gravity **3**(7), 193001 (2020)
62. G.N. Gadbail, S. Mandal, P.K. Sahoo, Physics **4**, 1403 (2022)
63. S. Perlmutter et al., Am. Astron. Soc. **2**(9), 1351 (1997)
64. A.V. Filippenko, A.G. Riess, Phys. Rep. **307**, 31 (1998)
65. M. Tegmark et al., Phys. Rev. D **6**(9), 103501 (2004)
66. D.N. Spergel et al., Phys. Rev. D **9**(1), 023518 (2015)
67. G.N. Gadbail et al., Eur. Phys. J. C **8**(3), 595 (2023)
68. A.S. Agrawal et al., Phys. Scr. **9**(7), 025002 (2022)